

# Evidence for charge orbital and spin stripe order in an overdoped manganite

H. Ulbrich,<sup>1</sup> D. Senff,<sup>1</sup> P. Steffens,<sup>2</sup> O.J. Schumann,<sup>1</sup> Y. Sidis,<sup>3</sup> P. Reutler,<sup>4</sup> A. Revcolevschi,<sup>4</sup> and M. Braden<sup>1,\*</sup>

<sup>1</sup>*II. Physikalisches Institut, Universität zu Köln, Zùlpicher Str. 77, D-50937 Köln, Germany*

<sup>2</sup>*Institut Laue-Langevin, BP 156, 38042 Grenoble Cedex 9, France*

<sup>3</sup>*Laboratoire Léon Brillouin, C.E.A./C.N.R.S., F-91191 Gif-sur-Yvette Cedex, France*

<sup>4</sup>*Laboratoire de Chimie des Solides, LPCES - ICMMO, Université de Paris Sud XI, 91405 Orsay, France*

(Dated: February 28, 2022)

Overdoped  $\text{La}_{0.42}\text{Sr}_{1.58}\text{MnO}_4$  exhibits a complex ordering of charges, orbitals and spins. Single-crystal neutron diffraction experiments reveal three incommensurate and one commensurate order parameters to be tightly coupled. The position and the shape of the distinct superstructure scattering points to a stripe arrangement in which ferromagnetic zigzag chains are disrupted by additional  $\text{Mn}^{4+}$  stripes. The observation of remarkably strong higher harmonics scattering for the orbital ordering corroborates this picture.

PACS numbers: 75.20.-m, 71.10.-w, 75.47.Lx, 75.50.Ee, 75.25.+z

In the stripe phases first observed in cuprates [1] additional charges segregate into stripes so that an anti-ferromagnetic order in between is conserved. The stripe scenario which can be considered as a soliton lattice is of general relevance in the physics of doped Mott insulators with similar stripe patterns being established in nickelates and in cobaltates [1–4]. The role of the orbital degree of freedom in manganites implies an additional aspect to stripe ordering as the magnetic interaction directly follows the orbital arrangement. Evidence of incommensurate ordering of charges and orbitals has also been observed for various manganites at higher doping levels, i.e. overdoped with respect to half doping with stable charge and orbital ordering (COO) but a clear picture of these phases, in particular the coupling to the magnetism, is still missing in spite of strong efforts [5–20].

First evidence for an incommensurate structural ordering in manganites was obtained from electron diffraction experiments which find the incommensurate modulations to linearly follow the amount of extra charges [5–7]. This fact was interpreted as evidence for stripe phases where the extra  $\text{Mn}^{4+}$  segregate into stripes along the diagonals of the simple perovskite lattice. In the meanwhile, numerous electron, x-ray and neutron diffraction experiments studied the stripe phases in various overdoped manganites, however, without reaching a clear conclusion [8–10, 13, 14, 18, 20]. So far it seems impossible to decide between the two proposed models: the Wigner crystal and the bi-stripe arrangement [5–7]. Furthermore, even the intrinsic nature of the structural phases remains matter of controversy. Both a soliton lattice reflecting the stripe pattern [11, 12] and a homogenous charge-density wave [13] have been proposed to explain the incommensurabilities generating strong controversy.

We have studied the charge, orbital and spin ordering (COSO) in overdoped  $\text{La}_{0.42}\text{Sr}_{1.58}\text{MnO}_4$  by single-crystal neutron diffraction. Three incommensurate order parameters associated with charges, orbitals and  $\text{Mn}^{3+}$  spins, respectively, and one commensurate one are tightly coupled with each other. The position and the shape of

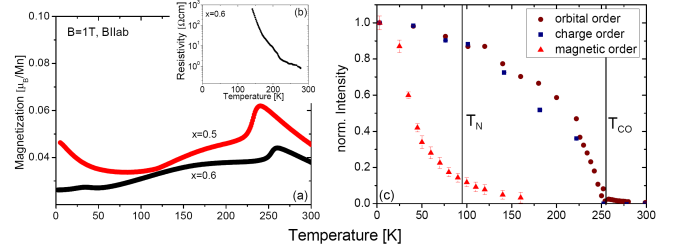


FIG. 1: Temperature dependence of magnetization as a function of temperature for a field of 1T applied parallel to the ab-planes for the half and for the overdoped compound (a). The inset presents the in-plane electric resistivity for  $x=0.58$  (b). Characteristic superstructure reflections measured by neutron diffraction increase in intensity at the transition temperature into the COO-state and into the AFM-state, respectively (c).

the different kinds of diffuse scattering as well as the observation of higher harmonics indicate a stripe-type arrangement where stripes of additional charges disrupt the ferromagnetic zigzag chains.

A large single crystal of  $\text{La}_{0.42}\text{Sr}_{1.58}\text{MnO}_4$  was grown by the floating-zone technique [23].  $\text{La}_{0.42}\text{Sr}_{1.58}\text{MnO}_4$  crystallizes in a tetragonal structure of space group  $I4/mmm$  with room-temperature lattice constants  $a_0=3.86$  Å and  $c_0=12.40$  Å. The magnetization was measured by a SQUID magnetometer and electric resistivity by a standard four-contact method (Fig. 1). The transition into the COO state ( $T_{CO}=255$ K) manifests itself by the appearance of superstructure reflections, as well as by a sharp drop of the magnetization  $M(T)$ . The antiferromagnetic ordering, however, is not visible in the macroscopic data most likely due to a strong 2D character. Magnetic superstructure reflections are detected below  $T_N \approx 95$ K in good agreement with [19], but the transition is sluggish. The neutron diffraction experiments were performed at the thermal diffractometer 3T.1 at the Laboratoire Léon Brillouin and at the triple-axis spectrometer IN20 at the Institut Laue Langevin. On 3T.1 we used a neutron energy of 14.7meV and two py-

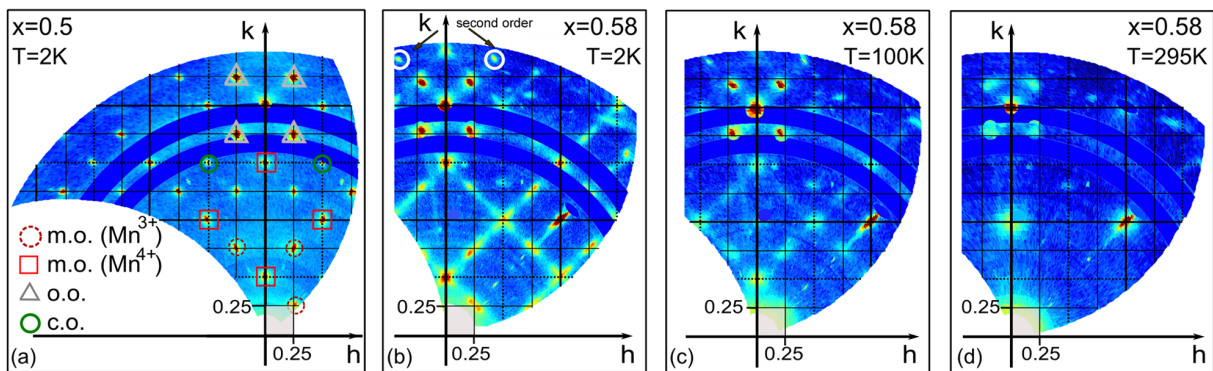


FIG. 2: Distribution of structural and magnetic scattering in the  $(h,k,0)$ -plane for  $\text{La}_{0.5}\text{Sr}_{1.5}\text{MnO}_4$  and  $\text{La}_{0.42}\text{Sr}_{1.58}\text{MnO}_4$ . For  $x=0.5$  superstructure reflections refer to the charge (green circles), orbital (grey triangles) and magnetic ordering ( $\text{Mn}^{3+}$ : dotted circles;  $\text{Mn}^{4+}$  red squares) (a). The COSO-state for  $x=0.58$  is governed by an incommensurate ordering of charge, orbital and magnetic ordering of  $\text{Mn}^{3+}$  (b). Slightly above the Néel-temperature  $T_N$  the magnetic superstructure reflections vanish but a diffuse magnetic signal is still visible (c). At room-temperature diffuse signals exist around the Bragg-reflections  $\mathbf{Q}=(0\ 2\ 0)$  and  $\mathbf{Q}=(0\ 1\ 0)$  (d). Contaminations from a crystallite and from the Al sample-holder are covered in blue color.

rolytic graphite (PG) filters to suppress higher order contaminations. On IN20 the flatcone detector with silicon (111) analyzers fixing the final energy to 18.7 meV allowed us to detect full maps of scattering in an efficient way. In all experiments, the  $c$ -axis was set vertical to the diffraction plane.

The COSO phase in  $\text{La}_{0.5}\text{Sr}_{1.5}\text{MnO}_4$  has been characterized in great detail using various scattering methods [18, 21, 24]. With the flatcone detector we may easily map the  $hk0$ -plane and identify the different types of characteristic scattering. With respect to the symmetry of the tetragonal high-temperature paramagnetic phase four different order parameters can be separated, see Ref. 24. Proper charge ordering of the checkerboard type is related to a mode at  $\mathbf{k}_{\text{co}} = \pm(0.5, 0.5)$  (referring to the 2-dimensional space and thus neglecting inter-layer coupling). The orbital ordering causes an additional doubling along one direction and is associated with a mode at  $\mathbf{k}_{\text{oo}} = \pm(0.25, 0.25)$ . The magnetism is described by two propagation vectors  $\mathbf{k}_{\text{Mn}^{3+}} = \pm(0.25, -0.25)$  and  $\mathbf{k}_{\text{Mn}^{4+}} = \pm(0.5, 0.0)$  referring to the nominal  $\text{Mn}^{3+}$  and  $\text{Mn}^{4+}$  spins, respectively. In the scattering map in Fig. 2(a) one may thus easily attribute each superstructure scattering with the associated order parameter. Just for the quarter-indexed peaks the identification is not intrinsic but can nevertheless easily be obtained due to the distinct  $\mathbf{Q}$ -dependence of magnetic and structural scattering.

Fig. 2(b) illustrates the same area of reciprocal space at  $T=2\text{K}$  for the overdoped system  $\text{La}_{0.42}\text{Sr}_{1.58}\text{MnO}_4$ . The single-counter scans across the different scattering types are shown in Fig. 3. The inspection of the two scattering maps immediately shows that the ordering phenomena in the two samples are qualitatively similar, but instead of the sharp signals at commensurate  $\mathbf{Q}$ -positions, there are broader features mostly centered at incommensurate positions in  $\text{La}_{0.42}\text{Sr}_{1.58}\text{MnO}_4$ . The direct comparison allows one to identify three underly-

ing ordering schemes. Superstructure reflections referring to the charge ordering are centered for example at  $\mathbf{Q}=(1.5+\delta_{\text{co}}\ 1.5+\delta_{\text{co}}\ 0)$  with  $\delta_{\text{co}}=0.080(3)$ . The incommensurability  $\delta_{\text{co}}$  does not change with temperature as scans parallel to the modulation exhibit only the thermal suppression of intensity, see Fig. 3(a). Fig. 2(b) demonstrates that the superstructure reflections associated with the orbital ordering are incommensurate, as well in agreement with previous x-ray experiments [18]. The orbital satellites are centered closer to the Bragg-reflection, for example  $\mathbf{Q}=(0\ 2\ 0)$  in diagonal direction. At this  $\mathbf{Q}$  range magnetic scattering can be fully neglected due to the magnetic form factor. The orbital scattering is incommensurately displaced towards the central Bragg peak,  $\mathbf{k}_{\text{oo}}=(0.25-\delta_{\text{oo}}, 0.25-\delta_{\text{oo}})$  and again there is no temperature dependency, see Fig. 3(b). The incommensurability of the orbital satellites is within the error bars exactly half of that of the charge ordering ( $\delta_{\text{oo}}=0.039(2)=\frac{1}{2}\delta_{\text{co}}$ ). These observations reveal the tight coupling between charge and orbital ordering in  $\text{La}_{0.42}\text{Sr}_{1.58}\text{MnO}_4$ , and they perfectly agree with previous diffraction studies on overdoped perovskite and bi-layer manganites using various diffraction methods [5–10, 13, 14, 18]. Most interestingly we clearly observe remarkably strong second-order harmonics of the orbital signal at  $(2,0,0)\pm 2\mathbf{k}_{\text{oo}}$ , see Fig. 2(b) and (c).

Inspection of Fig. 2(b) indicates that the quarter-indexed scattering associated with  $\text{Mn}^{3+}$ -spin ordering at half doping is split into two contributions in  $\text{La}_{0.42}\text{Sr}_{1.58}\text{MnO}_4$ . The incommensurate modulation of the  $\text{Mn}^{3+}$ -spin order is transverse with respect to the  $\text{Mn}^{3+}$  order in  $x=0.5$  (but note it is parallel to the chains)  $\mathbf{k}_{\text{Mn}^{3+}}=(0.25-\delta_{\text{Mn}^{3+}}, 0.25+\delta_{\text{Mn}^{3+}})$ , see Fig. 3(c). Scans in longitudinal direction yield a peak centered at the commensurate position due to the overlap of the two incommensurate contributions. As in Reference 19 only longitudinal scans were performed, the incommensurate character of the magnetic order was overlooked. The displace-

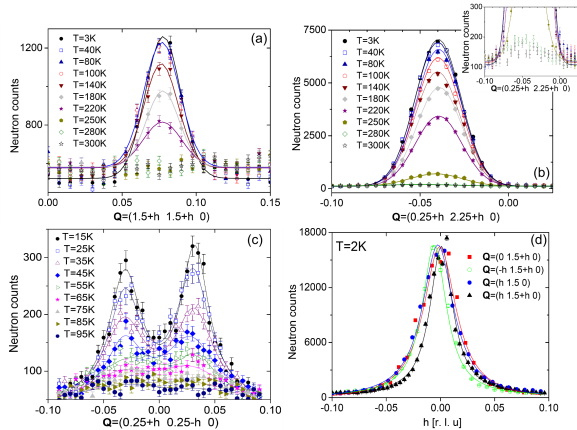


FIG. 3: Elastic scans across the positions of the different superstructure reflections. Satellites referring to the charge ordering (a) are displaced twice as much as those of orbital ordering (b) and of  $\text{Mn}^{3+}$  spin ordering (c), respectively. Reflections related to the magnetic ordering of  $\text{Mn}^{4+}$  appear at commensurate positions (d).

ment  $\delta_{\text{Mn}^{3+}}$  exhibits no temperature dependence. From several magnetic superstructure reflections we determine the average incommensurability  $\delta_{\text{Mn}^{3+}}$  which perfectly agrees with the incommensurability of the orbital ordering:  $\delta_{\text{Mn}^{3+}} = 0.037(2) = \delta_{\text{oo}} = \frac{1}{2}\delta_{\text{co}}$ . These three independent order parameters are all incommensurate and tightly coupled to each other.

The magnetic scattering associated with the ordering of  $\text{Mn}^{4+}$  spins are centered at the same positions as those in  $\text{La}_{0.5}\text{Sr}_{1.5}\text{MnO}_4$  (see Fig. 2), but the scattering in  $\text{La}_{0.42}\text{Sr}_{1.58}\text{MnO}_4$  exhibits diffuse tails along [110] direction. The commensurate ordering of  $\text{Mn}^{4+}$  spins appears astonishing as magnetic and orbital degrees of freedom are typically strongly coupled. Therefore additional scans were performed across the commensurate position  $\mathbf{Q}_{\text{Mn}^{4+}} = \pm(0.0, 1.5)$  in horizontal, vertical and diagonal directions. None of them indicates a sizeable incommensurability. Therefore we may safely exclude, that the  $\text{Mn}^{4+}$ -spin scattering exhibits an incommensurate shift comparable to those of the other three order parameters.

Because of an excess of  $\text{Mn}^{4+}$  ions an ideal checkerboard order of charges is not possible. The main question thus concerns the arrangement of these extra  $\text{Mn}^{4+}$ . Since all three observed incommensurabilities appear along the diagonal, these extra  $\text{Mn}^{4+}$  arrange in stripes along the diagonals as assumed already from the orbital reflections detected previously. This arrangement resembles the stripe phases observed in cuprates, nickelates and cobaltates [1–4] and corresponds to a soliton lattice. We may further deduce from the orbital incommensurate modulation, which is longitudinal in nature, that the disruption of the orbital order occurs along the zigzag-chains, or in other words that the  $\text{Mn}^{4+}$ -stripes align perpendicular to the chains. The magnetic superstructure reflections are in perfect agreement with this. The

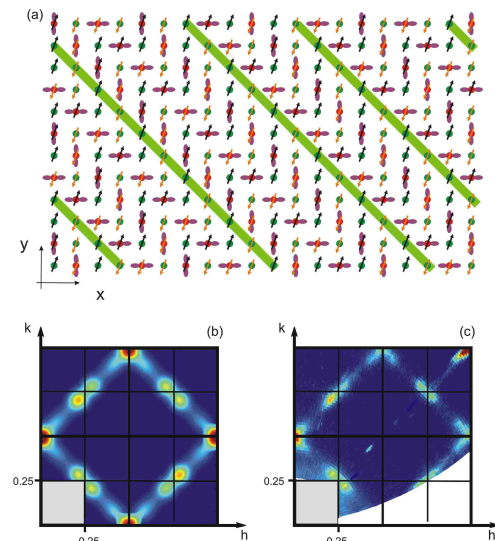


FIG. 4: Sketch of charge, orbital and spin order for  $\text{La}_{0.42}\text{Sr}_{1.58}\text{MnO}_4$  (a). Red circles represent  $\text{Mn}^{3+}$  and green circles  $\text{Mn}^{4+}$ . A single domain of zigzag chains propagating in [110] direction is shown. The excess lines of  $\text{Mn}^{4+}$  are displayed on a green background. The Fourier transformations map superposed for all domains (b) agree with the experimental map (c). Note, that the intensity at the position  $\mathbf{Q}=(1\ 1\ 0)$  in (c) is a Bragg peak.

magnetic propagation vector  $\mathbf{k}_{\text{Mn}^{3+}}$  points exactly perpendicular to the zigzag chains at half doping, so that the arrangement of the  $\text{Mn}^{4+}$  stripes perpendicular to the zigzag-chains results in a transverse modulation of the corresponding magnetic order. The resulting real-space model of this configuration is shown in Fig. 4.

It may appear astonishing that in spite of the stripe arrangement the magnetic scattering associated with the  $\text{Mn}^{4+}$ -spins at  $\mathbf{k}_{\text{Mn}^{4+}}$  remains commensurate, however, this fact is easily explained. The magnetic structure in the zigzag fragments can be constructed by following the strong ferromagnetic interaction across the  $\text{Mn}^{3+}$  orbitals. However, this does not fix the magnetic coupling in the double line of  $\text{Mn}^{4+}$ . Ferromagnetic  $\text{Mn}^{4+}$ -spin pairs in these double lines may align either horizontally or vertically (the vertical solution is shown in Fig. 4(a), but all these pairs must align in the same sense. The two possibilities, however, do not create distinct magnetic symmetries but only distinct domains; the symmetry of this magnetic structure is monoclinic generating thus four domain orientations with respect to the tetragonal high-temperature phase. This magnetic structure causes the commensurate  $\mathbf{k}_{\text{Mn}^{4+}}$  intensities, as the  $\text{Mn}^{4+}$ -spins sum up along the vertical bond direction and alternate in the horizontal direction resulting in magnetic scattering at  $\mathbf{Q}=(0.5, 0)$  for the domain chosen in Fig. 4.

In order to analyze the position and the shape of the different scattering contributions we performed two-dimensional Fourier-transformations of large supercells (typically  $380 \cdot 380$  lattices) in which the charge, orbital and spin order were implemented schematically. If we cal-

culate the average incommensurability of orbital, of magnetic ( $\text{Mn}^{3+}$ ), and half that of charge ordering, we obtain  $\delta=0.039(2)$  which via the scaling relation  $\epsilon(x)$  indicates a Sr content  $x=0.58$ . This value perfectly agrees with a single-crystal structure determination by x-ray diffraction, but is slightly below the nominal composition of the starting rod in the crystal growth [23]. The concentration  $x=0.58$  can not be realized by an adjustment of stripes with equal distances, but by a mixture of 33% blocks being arranged according to  $x=0.6$  and 66% blocks with  $x=0.57$ . The entire modulation consists thus of an alternation of blocks with seven lattice-spacings length and with five lattice-spacings length with a ratio of 2:1 [see Fig. 4(a)]. The structural arrangement consists thus of a soliton lattice in which only the average soliton distance is defined. The supercells of about 380-380 lattices are larger than the correlation lengths of the ordering in these manganites (and also larger than the neutron coherence length) so that finite-size effects can be neglected. The Fourier transformation fully explains the appearance of all the scattering observed, when the superposition of the four domains is taken into account [27]. The experimental maps indicate that the magnetic scattering is not sharp but exhibits diffusive tails along the diagonal concerning both the  $\text{Mn}^{4+}$  and the  $\text{Mn}^{3+}$  contributions; this effect is perfectly reproduced by the Fourier transformation as well. Magnetic order in the direction parallel to the stripes is perfect on a large length scale, but in the direction perpendicular to the stripes, magnetic order is regularly perturbed by the soliton generating diffuse tails. Such an anisotropic broadening was shown to yield direct evidence for a stripe arrangement [25]. The perfect agreement between the simulated and the experimental scattering maps including the diffuse tails gives strong evidence for the stripe arrangement and excludes a homogeneous spin and charge density wave modulation. This conclusion is further corroborated by the observation of the remarkably strong second-order harmonics of the orbital superstructure scattering, see Fig. 2(b), which exclude a simple sinusoidal density wave. The squaring up of a density wave is usually associated with third-order harmonics, but for the orbital pattern there is no squaring up but a strong pair or triple of opposite orbital phases (associated with a single "zig" in the chains) is surrounded by suppression of orbital order in the  $\text{Mn}^{4+}$  rows. This arrangement perfectly agrees with a strong second order harmonics. Evidence for a magnetic soliton arrangement in overdoped manganites was recently obtained by NMR experiments [17].

Above the onset of three-dimensional magnetic ordering at  $T_N \approx 95\text{K}$  we still observe a diffuse signal around the quarter- and half-indexed positions [see Fig.2(c)], but these signals rapidly lose intensity upon heating and a ferromagnetic signal increases in intensity [see Fig. 2(c)]. In the scattering map taken above the CO-state ( $T>T_{CO}$ ) the CE-type magnetic scattering is fully lost as it is also seen in the single-counter scans. The CE-type magnetic correlations get replaced by in-plane ferromagnetic cor-

relations centered around  $\mathbf{Q}=(0\ 1\ 0)$  [Fig. 2(d)] reflecting the increase of the macroscopic magnetization, see Fig. 1(a). The competition between the ferromagnetic short-range magnetic correlations and the CE-type low-temperature magnetic order reported for  $\text{La}_{0.5}\text{Sr}_{1.5}\text{MnO}_4$  [22, 24] thus persists in the overdoped concentration range.

The orbital and charge order scattering persists above  $T_N$  without any indication for a sizeable modification upon passing the magnetic transition. Although the charge scattering apparently fully disappears at the charge and orbital order transition, a sizeable amount of orbital scattering persists at  $T=295\text{K}$ , i.e. largely above the phase transition. This scattering is diffusive but it remains clearly incommensurate. The charge and orbital disordered state thus already exhibits the instability against incommensurate orbital ordering with the position fixed through the amount of doping. This incommensurate orbital instability cannot be directly caused by the magnetic correlations, as the orbital instability coexists with dominant ferromagnetic correlations [26].

In conclusion the position and the shape of the distinct types of superstructure scattering combined with the strong higher harmonics unambiguously indicate a stripe-like ordering in overdoped manganites.

This work was supported by the Deutsche Forschungsgemeinschaft through the Sonderforschungsbereich 608.

---

\* Electronic address: braden@ph2.uni-koeln.de

- [1] J.M. Tranquada *et al.*, Nature (London) **375**, 561 (1995).
- [2] J.M. Tranquada *et al.*, Phys. Rev. B **54**, 17 (1996).
- [3] R. Kajimoto *et al.*, Phys. Rev. B **64**, 144432, (2001).
- [4] M. Cwik *et al.*, Phys. Rev. Lett. **102**, 057201 (2009).
- [5] A.P. Ramirez *et al.*, Phys. Rev. Lett. **76**, 3188 (1996).
- [6] S.H. Chen *et al.*, J. Appl. Phys. **81**, 4326 (1997).
- [7] S. Mori *et al.*, Nature **392**, 473 (1998).
- [8] R. Wang and J. Gui, Phys. Rev. B **61**, 18 (2000).
- [9] T. Kimura *et al.*, Phys. Rev. B **65**, 020407 (2001).
- [10] J.C. Loudon *et al.*, Phys. Rev. Lett. **94**, 097202 (2005).
- [11] L. Brey and P.B. Littlewood, Phys. Rev. Lett. **95**, 117205 (2005); L. Brey, Phys. Rev. Lett. **92**, 127202 (2004).
- [12] G.C. Liward *et al.*, nature **431**, 607 (2005).
- [13] Z.P. Luo *et al.*, Phys. Rev. B **71**, 014418 (2005).
- [14] T.W. Beale *et al.*, Phys. Rev. B **72**, 064432 (2005).
- [15] X.Z. Yu *et al.*, Phys. Rev. B **75**, 174441 (2007).
- [16] A. Nucara *et al.*, Phys. Rev. Lett. **101**, 066407 (2008).
- [17] D. Koumoulis *et al.*, Phys. Rev. Lett. **104**, 077204 (2010).
- [18] S. Larochelle *et al.*, Phys. Rev. Lett. **87**, 095502 (2001).
- [19] S. Larochelle *et al.*, Phys. Rev. B **71**, 024435 (2005).
- [20] M. Pissa and G. Kallias, Phys. Rev. B **68**, 134414 (2003).
- [21] B.J. Sternlieb *et al.*, Phys. Rev. Lett. **76**, 2169 (1996)
- [22] D. Senff *et al.*, Phys. Rev. Lett. **96**, 257201 (2006).
- [23] P. Reutler *et al.*, J. Cryst. Growth **249**, 222 (2003).
- [24] D. Senff *et al.*, Phys. Rev. B **77**, 184413 (2008).
- [25] A.T. Savici *et al.*, Phys. Rev. B **75**, 184443 (2007).
- [26] I.V. Solov'yev, Phys. Rev. Lett. **91**, 177201 (2003).
- [27] Note, that there seems to be a slight imbalance in the domain occupation in the experimental map, and that we reduced the moment of the excess  $\text{Mn}^{4+}$ .